Mechanism and Effect of UCMSCS on Ovarian Structure and Function in Naturally Ageing C57 Mice

Xing-hua PAN
People's Liberation Army Joint Logistic Support Force 920th Hospital
Xue-juan ZHANG
People's Liberation Army Joint Logistic Support Force 920th Hospital
Xiang YAO
People's Liberation Army Joint Logistic Support Force 920th Hospital
Xiang-qing ZHU
People's Liberation Army Joint Logistic Support Force 920th Hospital
Jing ZHAO
People's Liberation Army Joint Logistic Support Force 920th Hospital
Jie HE
People's Liberation Army Joint Logistic Support Force 920th Hospital
Xue-min CAI
People's Liberation Army Joint Logistic Support Force 920th Hospital
Rong-qing PANG
People's Liberation Army Joint Logistic Support Force 920th Hospital
Guangping Ruan (✉ ruangp@126.com)
People's Liberation Army Joint Logistic Support Force 920th Hospital https://orcid.org/0000-0002-3784-7040

Research

Keywords: ovarian senescence, mUCMSC, follicles, granulosa cells, gene expression, apoptosis

Posted Date: June 8th, 2020

DOI: https://doi.org/10.21203/rs.3.rs-33308/v1

Abstract

Background: The ovary is the core reproductive organ of a woman and is of great significance for maintaining normal functioning of the reproductive system and the stability of the endocrine system. With an increase in age, the ovaries begin to age, and ovarian ageing will cause a decline in fertility.

Methods: Ageing C57 mice were used to explore the mechanism by which mouse umbilical cord mesenchymal stem cells (mUCMSCs) promote the antioxidant repair of granulocytes (mGCs). The ovarian volume in C57 mice, which were routinely reared to 18 months, decreased, and the follicles at all levels disappeared. All statistical analyses were performed using SPSS 21.0 statistical software. $P < 0.05$ was considered to indicate a significant difference.

Results: After mUCMSC transplantation, the mouse ovaries increased in size, follicles at various levels were seen in the cortex, and sinus follicle counts increased, indicating that mUCMSCs have a curative effect on ovarian ageing.

Conclusions: mUCMSCs downregulated the expression of apoptosis-related genes (Bax, Caspase-3), upregulated the expression of SOD2 and the peroxidase gene PRDX IV, and reduced the granulocyte apoptosis rate and ROS level. Co-cultivation with mUCMSCs can increase antioxidative stress in mGCs and reduce mGC apoptosis.

Introduction:

As is well known, female fertility declines with age. Since the 1960s, the development of contraceptive methods, the growth of economic wealth, the improvement in women's education level, and women's participation in the labour force have led many women to delay the birth of their first child [1, 2]. Due to the general trend of delayed fertility, increasingly more women that attempt to conceive will not be able to achieve this goal within 12 months. Thus, many couples rely on assisted reproductive technology (ART) to achieve pregnancy, but ART can only compensate for the decline in natural fertility to a limited extent [3], and many couples are still unable to have children after long-term infertility treatment. Female reproductive ageing is primarily based on age-related changes in ovarian function, which is dominated by the number of follicles present in the ovarian cortex and the gradual decline in oocyte mass within the follicles [4]. The ovary is the core reproductive organ of a woman and is of great significance for maintaining normal functioning of the reproductive system and the stability of the endocrine system. With an increase in age, the ovaries begin to age, and ovarian ageing will cause a decline in fertility. It also leads to a high risk of fractures and diseases, such as hot flashes, urogenital atrophy, and cardiovascular, cerebrovascular, and neuropsychiatric system diseases, during perimenopause[5–8], causing great harm to women's physical and mental health and bringing a severe economic burden to the family and society.

Normally, the reactive oxygen species (ROS) levels in the body are maintained in physiological balance under signal transduction and redox regulation, but high ROS levels can induce oxidative damage. In

normal cells, there is a complex antioxidant defence system that clears ROS and maintains the redox state of a variety of cells. However, as antioxidant levels decrease during ageing, leading to oxidative stress, the balance between ROS production and clearance is disrupted. Autophagy is a lysosomal-mediated self-digestion process that can maintain protein and organelle quality control. It is generally believed that ROS-induced autophagy increases during ageing, and oxidative stress is considered to be a major component of human ageing[9]. Therefore, autophagy is also involved in the ageing process.

Many studies have used mesenchymal stem cells to treat ovarian ageing. Li J et al.[10] used human umbilical cord mesenchymal stem cells (hUCMSCs) to treat naturally ageing rats. The results showed that hUCMSCs can secrete hepatocyte growth factor (HGF), vascular endothelial growth factor (VEGF) and insulin-like growth factor-1 (IGF-1) and can also promote the expression of the above three factors, thereby improving ovarian reserve function and mediating resistance to ovarian ageing. Ding C et al. [11] used human amniotic mesenchymal stem cells (hAMSCs) to treat naturally ageing mice and improved ovarian function in the naturally ageing mice.

Mesenchymal stem cells (MSCs) have become the most attractive cells for cell therapy due to their proliferative capacity, multidirectional differentiation, and paracrine effect and immunomodulatory properties. Collection of umbilical cord-derived mesenchymal stem cells is easy, painless and not ethically restricted; moreover, because sources are abundant and the cells have low immunogenicity, they have become the first choice for many mesenchymal stem cell applications. Umbilical cord mesenchymal stem cells (UCMSCs) have been used in a variety of disease models and achieved good results, including in a rat cerebral ischaemia model, Parkinson's disease, Alzheimer's disease, multiple sclerosis, retinal disease, autoimmune diseases, and type 1 and type 2 diabetes [12].

In this study, C57 mouse umbilical cord mesenchymal stem cells (mUCMSCs) were transplanted into naturally ageing C57 mice. The effects of mUCMSC transplantation were evaluated by observing mouse hair colour, ovarian index, hormone levels, ovarian tissue structure, and sinus follicle count. Granular cells in ovarian tissue were sorted for Smart-seq2 single-cell transcriptome sequencing, and the expression levels revealed by the granule cell transcriptome in the young control group, model control group, and treatment group were compared. Second, C57 mouse ovarian granulosa cells were cultured and used to establish a model of cell oxidative stress and then indirectly co-cultured with granulocytes using mUCMSCs to detect cellular reactive oxygen species (ROS) and apoptosis levels and evaluate whether mUCMSCs can promote granulocyte antioxidative stress. To repair oxidative damage, the results provide a valuable theoretical basis for use of UCMSCs to treat ovarian ageing.

Results:

1 Model selection and evaluation results

Compared with the young control group, the naturally ageing C57 mice (18 months) had a disordered oestrous cycle and ovarian atrophy, and the ovarian parenchyma was occupied by interstitial cells. No

follicles were seen at any levels, and serum INH-B levels were reduced ($P < 0.05$). These findings met the ovarian ageing characteristics, and thus, 18-month-old C57 mice were used as the female ovarian natural ageing mouse model.

2 Mucmsc Growth Morphology

Umbilical cord tissue from the mice cut to no obvious tissue block was evenly spread in a 10 cm petri dish. On the second day, a small number of cells around the tissue block could be observed to climb out and showed a short spindle shape (Fig. 1A). As time progressed, more cells appeared in colonies around the tissue mass, covering 80% of the bottom of the dish (Fig. 1B), and the cells could be passaged at this time. The mUCMSCs were digested by trypsin with different digestion times. The mixed cells still remained on the bottom of the culture dish. When passaged to the 3rd to 5th generations, the mUCMSCs were spindle-shaped, with a fibroblast-like and uniform morphology (Fig. 1C).

3 Immunophenotype Of Mucmscs

Flow cytometry results showed that the positive expression rates of the mUCMSC surface antigens CD29, CD90, and CD34 were 98.6%, 100%, and 0.39%, respectively, and the isotype control was negative, consistent with the phenotypic characteristics of umbilical cord mesenchymal stem cells. The results (Fig. 1D) are as follows.

4 Mucmsc Multipotent Differentiation Potential

Fourth generation mUCMSCs were used to perform in vitro differentiation experiments, and the differentiation time was 14–21 days. The negative control is shown in Fig. 1E. After osteogenesis induction, alizarin red staining was performed, and red-stained calcium nodules appeared. The positive rate was approximately 98% (Fig. 1F). After adipogenic induction, staining with oil red O showed red-stained lipid droplets, with a positive rate of approximately 90% (Fig. 1G). After cartilage induction and staining with Alcian blue, proteoglycans synthesized by blue-stained chondrocytes appeared, and the positive rate was approximately 95% (Fig. 1H).

5 Mucmsc Gfp Labelling And Tracing

Third generation mUCMSCs were labelled with GFP and observed under an optical microscope (see Fig. 1I). Under fluorescence excitation, most cells exhibited bright green fluorescence (see Fig. 1J). The positive rate of GFP detection by flow cytometry reached 100% (Fig. 1M). One month after the GFP-labelled mUCMSCs were injected into the mice, a green fluorescent cell (see Fig. 1K) was seen in the ovarian tissue under a fluorescence microscope. GFP-labelled mUCMSC-positive cells (Fig. 1L) were observed after DAPI staining. The proportion of positive cells was approximately 5%, concentrated in the

ovarian cortex, indicating that UCMSCs injected into the tail vein of mice could migrate to the mouse ovaries.

6 Growth Morphology And Identification Of Mgcs

6.1 mGC growth morphology

mGCs were adherently cultured, and the primary morphology was short-fusiform, with a uniform size (Fig. 2A), but after passage to the P1 generation, the morphology became uneven in size (Fig. 2B). Granular cells are not easy to culture, and the passage cannot exceed 3 generations. During the experiment, the adherence rate of P2 generation cells was significantly reduced, and the cells easily died and floated. Therefore, P1 generation mGCs were used in subsequent experiments.

6.2 Mouse Ovarian Granulosa Cell Identification

C57 mouse ovarian granulosa cells were identified by immunofluorescence, and the purity of the cells was above 90% (see Fig. 2C-2F).

7 Efficacy Evaluations

7.1 Mouse hair colour change

After mUCMSC transplantation, the hair colour of C57 ageing mice recovered, becoming darker and brighter, and the gloss was significantly improved (see Fig. 2G). ImageJ software was used to calculate the hair colour of each mouse in the three groups in the same area of the neck, back and tail. The degree value and the grey value of the hair colour in the treatment group were significantly higher than those in the model control group ($P < 0.05$) (see Fig. 2H).

7.2 Mouse Ovarian Index

The mouse ovarian index is the ratio of ovarian weight to mouse weight. Compared with the model control group, the ovarian index in the treatment group increased ($P < 0.05$) (Fig. 2I).

7.3 Endocrine Changes

Compared with the model control group, the levels of serum oestrogen (E2), inhibin B (INH-B), and anti-Müllerian tuberculosis hormone (AMH) in C57 mice were significantly increased after treatment ($P < 0.05$). There was no difference in hormone (FSH) levels ($P > 0.05$) (Fig. 2J-2M).

7.4 Ovarian Histological Changes

Gross observation: The ovary size in the young control group of C57 mice was approximately 6 × 3 × 3 mm, showing a flesh colour. The ovaries of C57 mice in the model control group were smaller, approximately 1 × 1 × 1 mm in size, darker in colour, and reddish brown. After transplantation, the ovaries increased to approximately 4 × 2 × 2 mm in size, and the colour returned to light red (see Fig. 3G). In the young control group, the ovarian structure observed under a light microscope after HE staining was intact, and the follicular structure at each level of the ovary was clear (Fig. 3A). After magnification (Fig. 3B), preantral sinus follicles (black dotted arrows) and sinus follicles (black thick arrows) were visible. The ovarian structure in the model control group was completely lost, and no follicular structure was seen at any levels (Fig. 3C). After zooming in (Fig. 3D), a large number of primitive follicles and granulosa cells were found to be swollen, necrotic and disintegrating, and the nuclei were condensed (black thick arrow). In addition, a small amount of inflammatory cell infiltration (black thin arrow) and a small amount of brownish-yellow pigment deposition (black dotted arrow) was observed. After the mUCMSC treatment, the ovarian structure was complete, the structure was clearer, and the follicles and corpus luteum structure were visible at all levels in the ovary. There were more atresia follicles, and the inferior sinus follicles (black thick arrows) and atresia follicles (black thin arrows) were significantly improved (see Figs. 3E and F). The follicles at all levels were counted. Compared with the model control group, the number of original follicles was elevated. The model control group had no primary follicles, secondary follicles, or sinus follicles. After treatment, primary follicles, secondary follicles, and sinus follicles appeared. Atretic follicles were increased compared with the model control group (Fig. 3H).

8 Changes In Protein Expression Of Ovarian Ageing-related Genes

8.1 Changes in protein expression of the ageing-related genes P53, P16, SOD1

P53 gene protein expression was higher in the young control group, lower in the model control group, and lower in the treatment group after treatment ($P > 0.05$). P16 gene protein expression was lower in the treatment group than in the model control group ($P < 0.05$). SOD1 gene protein expression was higher in the model control group than in the young control group and was significantly decreased after treatment ($P < 0.01$) (Fig. 4). The mouse-derived ovarian senescence-related gene cloning and amplification primers were designed and synthesized by Wuhan Saiweier Biotechnology Co., Ltd. (Table 1).

Table 1
Primer information for 13 ovarian ageing-related genes

Gene ID Gene name	Primer sequence (5'→3')	Product length (bp)	Annealing temperature (°C)
NM_001127233.1 (P53)	F:ATGAACCGCCGACCTATCCT	264	60.76
	R: GCGGATCTTGAGGGTGAAATAC		59.13
NM_013671.3 (SOD2)	F:TCCCAGACCTGCCTTACGACT	244	61.1
	R: CCCTTAGGGCTCAGGTTTGTC		60.4
NM_009810 (CASP3)	F:GTCTGACTGGAAAGCCGAAAC	205	58.9
	R: GACTGGATGAACCACGACCC		59.5
NM_007527 (Bax)	F: GCCTTTTTGCTACAGGGTTTCAT	151	61.9
	R: TATTGCTGTCCAGTTCATCTCCA		59.9
NM_009741.5 (Bcl2)	F: GCTACCGTCGTGACTTCGCA	270	61.9
	R: CATCCCAGCCTCCGTTATCC		61.6
NM_019584.3 (becline1)	F: GCAGCAGTTCAAAGAAGAGGTG	122	60.3
	R: TTTTGATGGAATAGGAGCCGC		58.7
NM_026160.4 (LC3b)	F: CGTCCTGGACAAGACCAAGTTC	80	61.12
	R: GCAAGCGCCGTCTGATTATC		59.77
NM_001159589.1 (sirt1)	F: CAGCATCTTGCCTGATTTGTAA	268	57.29
	R: TGGGGTATAGAACTTGGAATTAGTG		58.1
NM_011034.4 (PRDXI)	F: CCACGGAGATCATTGCTTTCA	139	58.64
	R: GGCCCAATCCTCCTTCTTTC		58.55
NM_001313711.1 (PRDXIV)	F: TGTTGCGGACCGAATCTCTG	178	60.39
	R: CAATAAGGTGCTGGCTTGGAGA		60.62

Gene ID Gene name	Primer sequence (5'→3')	Product length (bp)	Annealing temperature (°C)
NM_001358444.1 (PRDXV)	F: AAGAAGCAGGTTGGGAGTGTG R: AACAGCCAGGTGTAAATGCCC	201	60.48 61.17
NM_001303408.1 (PRDXIVI)	F: CACCACAGGAACTGGCAGAC R: TGGTGGCAGGGTAGAGGAAG	317	61.47 60.41
NM_007393.3 (β-actin)	F: GTGACGTGACATCCGAAAGA R: GTAACAGTCCGCCTAGAAGCAC	287	58.7 61.0

8.2 Changes in protein expression of the autophagy-related genes becline1, LC3b, Sirt1, Sirt3, and P62

The protein expression of the autophagy-related genes becline1 and LC3b was lower than that in the model control group after treatment ($P < 0.05$), and Sirit3 expression was significantly higher than that in the model control group ($P < 0.05$). The protein expression of sirt1 and p62 was not significantly different (Fig. 5).

8.3 Protein expression changes in the apoptosis-related genes Bax, Bcl-2, and Caspase3 and in granular cell FSHR

After treatment, protein expression of the apoptosis-associated gene Caspase-3 was significantly lower than that in the model control group ($P < 0.05$). The protein expression of other apoptosis-related genes, Bax and Bcl-2, was not significantly different, and the expression level of the granulocyte-specific protein FSHR in the treated group was lower than that in the model control group ($P < 0.05$) (Fig. 6).

9 Changes In Ovarian Apoptosis

The positive rate of TUNEL staining in the model control group was higher than that in the young control group ($P < 0.05$). After treatment, the positive rate of TUNEL staining in the ovary was lower than that in the model control group ($P < 0.05$) (Fig. 7A-G).

10 Transcriptome Expression Levels Of Ovarian Ageing-related Genes

Compared with the young control group, the expression of the ageing-related gene P53 in the model control group was decreased ($P < 0.05$) (Fig. 7H). SOD2 expression was higher in the young control group, decreased after ageing, and increased after mUCMSC treatment ($P < 0.05$) (Fig. 7I). Ovarian expression of the apoptosis-related genes Bax and Caspase-3 increased in the model control group and decreased after mUCMSC treatment ($P < 0.05$) (Fig. 7J). The expression of the autophagy-related gene LC3b was higher in the model control group than in the young control group, and the expression was downregulated after treatment ($P < 0.05$) (Fig. 7K). The expression of the peroxidase gene PRDXI was increased in the treatment group compared with the model control group ($P < 0.05$). The expression of PRDX IV in the ageing ovary decreased but was upregulated after treatment ($P < 0.05$), and PRDX VI was downregulated in the ageing ovary ($P < 0.05$) (Fig. 7L).

11 Granular Cell Sequencing Results

11.1 Granular Cell Sorting Results

Granulocyte-specific FSHR antibodies were used to sort ovarian granulosa cells via flow cytometry, with a positive rate of 99% on average (Fig. 7M).

11.2 Granular Cell Sequencing Results

11.2.1 Principal Component Analysis of Granular Cell Gene Expression in Three Groups

Principal component analysis (PCA) of gene expression was performed to investigate the distribution of samples, explore the relationship between samples, or verify the experimental design. PCA can show the relationship between samples from different dimensions. The closer the sample clustering distance or PCA distance is, the more similar the samples are. Each group of samples was distributed in two different areas, and the samples in the same group were more concentrated in space. The PCA chart (Fig. 8A) is shown below.

11.2.2 Granular Cell Differential Expression

A total of 707 differentially expressed genes were detected in the ovarian granulosa cells from the model control group and the youth control group, of which 272 were upregulated and 435 were downregulated. Overall, 832 differentially expressed genes were detected in the granulocytes of the mUCMSC treatment group and the model control groups, of which 277 genes were upregulated and 555 were downregulated.

In clustering, the same types of samples appear in the same cluster. Protein-coding genes clustered in the same cluster may have similar biological functions. A sequencing sample cluster map was obtained based on the differential gene expression (see Fig. 8B and 8C).

11.2.3 Go Enrichment Analysis Of Granular Cell Differential Genes

GO enrichment analysis of the top 30 (screening for GO entries with a number of corresponding differential genes greater than 2 in the three classifications, 10 entries from the -log10 P value in descending order of each entry) was performed, bar graphs were constructed (as shown in Figs. 9A, 9B and 9C, 9D). Wayne analysis was performed on the young control group and model control group and the mUCMSC treatment group and model control group (Fig. 9E). Eleven common differences were obtained (Table 2). Immune response and inflammatory response were selected. The comparison between the youth control group and the model control group involved 31 immune response genes; 21 genes were involved in the immune response entry in the mUCMSC treatment group and the model control groups according to Wayne analysis (Fig. 9F), and the gene participating in the immune response entry was Tnfaip3. In the youth control group and the model control group, 50 genes were involved in the inflammatory response entry in the comparison, and 15 genes were involved in the inflammatory response entry in the mUCMSC treatment group and the model control group. According to the analysis (Fig. 9G), 8 genes were involved in the inflammatory response entry, namely, Slc11a1, Smpdl3b, Tlr13, Naip6, Cysltr1, Csf1r, Tlr8, and Tnfrsf11a. The 8 genes were queried in the string network to obtain a string diagram (Fig. 9H).

Table 2
GO analysis of three sets of common difference entries

Term	Model vs control	mUCMSC vs model
immune system process	up	down
innate immune response	up	down
immune response	up	up
inflammatory response	up	down
external side of plasma membrane	up	down
MHC class I protein binding	up	down
membrane	up	down, up
plasma membrane	up	down, up
cell surface	up	down, up
protein binding	up	up
apical plasma membrane	down	up

11.2.4 Kegg Enrichment Of Granular Cell Differential Genes

Pathway analysis of differentially expressed genes can be used to find Pathway entries enriched for differentially expressed genes and to find which cellular pathways may be related to the protein encoding genes differentially expressed in different samples. KEGG enrichment analysis of the top 20 genes (screening for pathway entries corresponding to a number of differentially expressed genes greater than 2, according to the -log10 P value of each entry, sorted from large to small) is shown in a bubble chart (as shown in Fig. 10A and Fig. 10B). The larger the bubble entry is, the greater the number of differentially expressed protein-coding genes. The colour of the bubbles changes from purple to blue to green to red, and the smaller the enrichment p value is, the greater the significance is. Wayne analysis was performed on the differential pathways between the young control group and model control group and the mUCMSC treatment group and model control group (Fig. 10C); a total of 10 identical pathways were found (Table 3).

Table 3
Common differential pathways from KEGG pathway analysis

Term	Model vs control	mUCMSC vs model
Osteoclast differentiation	up	down
Chemokine signalling pathway	up	down
Tuberculosis	up	down
NOD-like receptor signalling pathway	up	down
Natural killer cell mediated cytotoxicity	up	down
Platelet activation	up	down
Cytokine-cytokine receptor interaction	up	down, up
TNF signalling pathway	up	up
PI3K-Akt signalling pathway	down	up
ECM-receptor interaction	down	up

11.2.5 Analysis of Differential Gene mRNA Trends in Three Groups of Granular Cells

With clustering, the same types of samples appear in the same cluster. The protein-coding genes clustered in the same cluster may have similar biological functions. Three sets of cluster analysis heat maps were constructed (Fig. 10D). The trend map showed 299 differentially expressed genes in three groups in Trend 6 (Fig. 11A). The GO level 2 distribution map of the top 30 differentially expressed genes in Trend 6 (Fig. 11B) and the Top 30 distribution of Gene KEGG Analysis in Trend 6 (Fig. 11C) show that the genes are primarily involved in regulating cell population proliferation, the P53 signalling pathway, the P13k-Akt signalling pathway and insulin-like growth factor binding proteins (IGFBPs) in insulin-like growth factor (IGF) transport and uptake.

12 Analysis Of Mucmsc Antioxidant Levels

12.1 Mouse ovarian granulosa cell oxidative stress model

C57 mouse ovarian granulosa cells were treated with H_2O_2. Granulocytes were put in a hypoxic environment, and the oxidative stress protection mechanisms of the granulocytes were stimulated. Under hypoxic conditions, the ROS levels in the mGCs increased ($P < 0.05$).

12.2 Ros Level In Mgcs

After H_2O_2 treatment, the ROS level in ovarian granulosa cells from C57 mice increased. After indirect co-culture with mUCMSCs, the ROS level in the cells decreased significantly (Fig. 11D, 11E).

12.3 Mgc Apoptosis Level

Flow cytometry was used to detect apoptosis of granular cells. Co-culture with mUCMSCs significantly reduced early and late apoptosis (Fig. 11F).

12.4 Transcription levels of the apoptosis-related genes Bax and Bcl-2

qRT-PCR was used to detect the transcription level of apoptosis-related genes in granule cells. The results showed that mUCMSCs reduced the expression of the apoptotic gene Bax and upregulated the expression of the antiapoptotic gene Bcl-2 (Fig. 11G).

Discussion:

1 Evaluation of ovarian ageing model

The main functions of the ovary are ovulation and secretion of hormones. The number of follicles in the ovary is limited. At 20 weeks of gestation, the number of original follicles can reach 6 million to 7 million, which will gradually decrease in later years, reaching 300,000 to 400,000 by puberty and dropping to approximately 1,000 after menopause. In addition, 12 to 14 years after menopause, the number is eventually depleted by atresia and apoptosis[13]. On average, approximately 400–500 mature egg cells are excreted in the life of a normal woman, and most of the follicles degenerate and lock at various stages of development. With age, in addition to the decrease in the number of follicles, the quality of oocytes also decreases.

Animal models of ovarian ageing at home and abroad include natural ageing models and induced ageing models. Ding C et al. [11] used 12- to 14-month-old female mice as ageing models. Jia Li et al.[10] used 12- to 14-month-old female SD rats, and the oestrous cycles were observed to determine cycle disorder as a model. Induced ageing models mainly employ superovulation to accelerate ovarian ageing. Zhang J et al. [14] induced superovulation and ozone inhalation in female mice to establish ovarian ageing models. Establishment of the appropriate animal model is the key to a successful study. Because the present study focused on natural ageing, animals with natural ageing were used.

In this study, C57 naturally ageing mice were used. This laboratory primarily studies UCMSCs for treatment of ageing-related diseases. Since this study successfully established and identified a natural ageing C57 mouse model, it was directly selected according to the previous model. Female C57 mice aged 72 w were used as a model of ovarian ageing. During the normal fertility period, the menstrual cycle proceeds regularly. When the menopausal transition period begins, the regularity of the menstrual cycle is gradually lost, which indicates that the ovaries are beginning to age. In mice, the oestrous cycle is

equivalent to the human menstrual cycle. Vaginal smears were evaluated to compare the oestrous cycle of young and old mice. The oestrous cycle of old mice was disordered. Therefore, mice with oestrous cycle disorders were included in the group as an animal model of ovarian ageing.

2 Mucmscs For Cell Transplantation

In many studies, the stem cells used to treat ovarian ageing are human umbilical cord mesenchymal stem cells [10], human amniotic mesenchymal stem cells [11], or human fat-derived mesenchymal stem cells [15]. No one has used a mouse model and adopted mouse umbilical cord mesenchymal stem cells (mUCMSCs). Although studies have shown that mesenchymal stem cells have very low immunogenicity and will not cause immune rejection, homologous mesenchymal stem cells can be used for treatments. However, the differences in heterogeneity are not specifically quantified, and the differences between humans and mice are obvious. To exclude the effects of species differences, mouse umbilical cord mesenchymal stem cells were used in this study. The animal model was C57 mice. Umbilical cord mesenchymal stem cells were also taken directly from young C57 mice.

Young C57 mice are small in size and weigh approximately 19–25 g. The umbilical cord taken from pregnant mice is particularly small, approximately 1–2 cm long, and surrounded by a membrane, and because the umbilical cord is small and easily torn, blood in the umbilical cord cannot be completely removed. Therefore, primary culture can first retain a portion of the tissue around the umbilical cord and squeeze the blood, but not strictly. After preliminary explorations, it was found that mUCMSCs can be digested with 0.25% trypsin for 1 min, but the time cannot exceed 1 min. This can largely reduce the number of miscellaneous cells and allow passage to the third generation, and the basic purity of mUCMSCs can reach more than 90%. From morphology assessment, induced differentiation, and flow cytometry identification, the mUCMSCs cultured in this study were found to meet the standards for umbilical cord mesenchymal stem cells and can be used for cell transplantation.

3 Evaluation Of Mucmsc Transplantation

First, one month after GFP-labelled mUCMSCs were injected into mice, green fluorescent cells could be observed in mouse ovarian tissue under a fluorescence microscope, indicating that mUCMSCs injected through the tail vein can migrate and home to mouse ovaries.

Second, the efficacy of transplantation was evaluated from the following aspects. First, the hair colour of the mice was compared, and the hair colour of the model group became dark, with many white hairs also present. After treatment, the mouse hair colour became black and bright, with no white hair. Second, general and structural observation of ovarian tissues showed that the ovaries atrophied and became smaller after ageing, and the ovaries were substantially occupied by interstitial cells. The ovarian structure was completely lost, and follicles and granule cells could not be seen at any level. Swelling, necrosis, and a small amount of inflammatory cell infiltration were also seen. After mUCMSC treatment,

the ovary volume became significantly larger, the ovarian structure became intact again, and follicles could be seen at all levels. After mUCMSC treatment, the ovarian reserve function was significantly improved. If the reproductive ability of mice can be further observed to improve after treatment, then mUCMSCs can delay or even reverse ovarian ageing.

Third, it is about the changes in mouse hormones. In addition to anti-Müllerian hormone (AMH), evaluation of ovarian function takes into account oestradiol (E2), follicle stimulating hormone (FSH), and inhibin B (INH-B) levels. In this study, E2 and INH-B were significantly higher in the treatment group than in the model group, indicating that after mUCMSC treatment, ovarian function was improved, and follicles of various levels, including sinus follicles, appeared. Granular cells of sinus follicles could secrete E2 and INH-B, but the FSH decrease was not significant. It is speculated that the mice developed a regular oestrous cycle after the improvement in ovarian function, but the time when the FSH level of the mice was raised was encountered during the collection, and thus, the effect of reducing FSH was not obvious.

4 Possible mechanisms by which mUCMSCs improve ovarian function in aged mice

The two factors that affect ovarian ageing are a decrease in the number of follicles and a decrease in the quality of oocytes. The decrease in the number of follicles results from acceleration of the rate of recruitment of primitive follicles and an increase in the number of atretic follicles. On the other hand, the increase in the aneuploidy of oocytes with ageing is caused by a decrease in the mass of granulocytes around the oocytes.

There are many reports at home and abroad on treatment of ovarian ageing with mesenchymal stem cells. Jia Li[10] used human umbilical cord mesenchymal stem cells (hUCMSCs) to treat 12-to 14-month-old SD rats and found that hUCMSCs can not only secrete hepatocyte growth factor (HGF), vascular endothelial growth factor (VEGF) and insulin-like growth factor (IGF-1), they can also promote the expression of the above three factors. The results of this experimental study showed that the expression of the autophagy-related gene LC3b was increased in the ovarian tissue of ageing mice and decreased after treatment with mUCMSCs, indicating that autophagy was enhanced in ageing mice. Moreover, ovarian tissue recovered after treatment, autophagy was reduced, and autophagy-related gene expression also decreased.

In this study, combined with the immunohistochemistry and qRT-PCR results, it was shown that the ovarian superoxide dismutase SOD1, the autophagy-related gene LC3b, the granulocyte apoptosis-related gene Bax, and the apoptosis-related gene Caspase-3 were upregulated in the model group. After treatment, expression was downregulated, while superoxide dismutase SOD2 and peroxidase PRDX IV expression levels were downregulated in the model group and upregulated after treatment. Second, TUNEL staining of ovarian tissue showed that with age the rate of apoptosis in ovarian tissue increased and mUCMSCs could reduce the apoptosis rate. Therefore, it is speculated that mUCMSCs may improve ovarian ageing by reducing oxidative stress and ovarian cell apoptosis.

In this study, Sirt3 was significantly increased after mUCMSC treatment. It is speculated that Sirt3 is involved in promoting ovarian repair.

5 Ovarian Granulosa Cell Transcriptome Sequencing Analysis

Follicles are composed of oocytes and two somatic granule cells and follicular membrane cells surrounding the oocytes, which play a major role in steroid production. Granular cells proliferate and secrete steroid hormones in response to several stimuli, such as FSH and LH, and therefore play an important role in follicular development [16]. Due to insufficient survival signals and / or physiological / non-physiological apoptotic signals, granule cells lead to follicular atresia apoptosis [17, 18].

At present, sequencing and analysis of ovarian granulosa cells is primarily focused on tumours, and there is little research on ageing. There is no research on the isolation and sequencing of mouse ovarian granulosa cells.

Ovarian granulosa cells are surrounded by oocytes, and thus, the quality of granulocytes will affect oocyte development. Therefore, this study was designed to screen genes and signalling pathways that affect ovarian granulosa cells by comparing mRNA differences in ovarian granulosa cells from each group. In this study, GO enrichment analysis of differential gene functions mainly included inflammatory response, immune response, cytokine and cytokine receptor activity, cell surface components, and protein binding. Compared with the young control group, the expression levels of genes regulating the inflammatory response and immune response were upregulated in ovarian granulosa cells from the model control group. After mUCMSC treatment, genes regulating the inflammatory response and immune response were downregulated. UCMSCs have anti-inflammatory activity and regulatory immunity. They can also promote tissue repair through paracrine cytokines, which is consistent with the results of this study. It can be concluded that UCMSCs can improve the quality of ovarian granulosa cells via anti-inflammatory activity and by regulating immunity and provide protection for oocyte quality.

Analysis of KEGG pathways revealed that the differential pathways include the chemokine signalling pathway, the NOD-like receptor signalling pathway, natural killer cell-mediated cytotoxicity, and cytokine-cytokine receptor interaction, TNF signalling pathway upregulation, the PI3K-Akt signalling pathway, and the ECM-receptor interaction pathway. A STEM trend analysis of three groups was performed to obtain 81 differentially expressed genes, all of which were downregulated from young mice to old mice and then upregulated after treatment. The 81 genes were queried on the string network and were mainly involved in regulating cell population proliferation, the P53 signalling pathway, the P13k-Akt signalling pathway and insulin-like growth factor binding proteins (IGFBPs) in insulin-like growth factor (IGF) transport and uptake.

Experimental Procedures:

1 Screening and evaluation of ovarian ageing model in C57 mice

Weitong Lihua purchased 50 female C57 mice at 8 days and 8 months of age (weighing (15 ± 2.5) g and (20 ± 5) g) and raised them on conventional feed until 2 months and 18 months, respectively. For 30 days, three vaginal smears were taken for observation, and three eyeballs were taken to test for serum oestradiol (E2), follicle maturation hormone (FSH), anti-Müllerian hormone (AMH), and inhibin B (INH-B) levels in the blood. The cervical spine was sacrificed. Paraffin-embedded sections of ovarian tissue were examined by HE staining, ovarian structure was observed, and sinus follicles were counted.

2 Preparation And Identification Of Mucmscs

Eight pregnant C57 mice were collected at 18 days of pregnancy. The mouse umbilical cord was collected under in vitro aseptic conditions and cultured with tissue blocks, and then, adherent mUCMSCs were purified by trypsin digestion, and the morphology was observed under a microscope. CD29, CD34, and CD90 expression was analysed via flow cytometry. The mUCMSCs were induced to differentiate into osteoblasts, adipocytes and chondrocytes, and their differentiation potential was analysed.

GFP labelling of mUCMSCs: First, the optimal MOI value (referring to the number of viruses infected by each cell) determine to be 100. The P3 generation of mUCMSCs was plated into a six-well plate. Coverslips were placed at the bottom of two wells. The coverslips were wiped with alcohol, baked with an alcohol lamp, and cooled. When the fusion rate reached 80%, Shanghai Jiman Biological CMV-Luciferase-EGFP-Puro lentivirus was added along with the transfection reagent polybrene to a final concentration of 5 μg / ml. The solution was changed after 8 hours. After 48 hours, the coverslip was placed on a glass slide, and the cells were fixed with 4% paraformaldehyde for 30 min. The expression of GFP was observed under a fluorescence microscope. The cells in the remaining wells were digested into a cell suspension and washed twice. The precipitate was resuspended in PBS and divided into flow tubes (100 μl / tube), and 300 μl PBS was added. A flow cytometer was used to detect the positive rate of GFP expression.

3 C57 mouse ovarian granulosa cell (mGC) culture and identification

Primary mGCs were purchased and placed in a cell incubator at 37 °C and 5% CO_2 for 4 hours after sterilization. Then, the complete medium filling the T25 flask was halved, and the culture was continued in the incubator. The next day, half of the solution was exchanged with C57 mouse ovarian granulocyte special medium. When cell fusion reached 80%, the cells were digested with 0.25% trypsin (2 ml) for 1 min, and then, special mGC medium (4 ml) was used to terminate the digestion. The cells were collected into a 15 ml centrifuge tube and centrifuged at 300 × g for 5 min, and the pellet was resuspended in 2 ml of special mGC medium. T25 culture bottles were then filled with 4 ml of special mGC medium and 1 ml of cell suspension. Cells were placed into climbing slides, identified with rabbit

anti-mouse follicle stimulating hormone receptor (FSHR) antibody, observed with a fluorescence microscope, and photographed.

4 Mucmsc Treatment

Briefly, 18-month-old C57 mice were randomly divided into a model control group and a treatment group. At the same time, 2-month-old C57 mice were set as a young control group, with 15 mice in each group. The treatment group was injected with GFP-labelled mUCMSCs via the tail vein (1×10^7 / kg, volume 100 μl, injected every Monday and Thursday for 3 consecutive weeks). The model control group was injected with the same volume of normal saline. The young control group received no treatment. One month after the last injection of mUCMSCs, the treatment efficacy was evaluated, and the mechanism was studied.

5 Evaluation Of Mucmsc Transplantation

The mouse coat colour was observed, and the mouse ovarian index was calculated. ELISAs were conducted to detect serum E2, FSH, AMH and INH-B levels. Gross dissection was performed to observe ovarian shape and size, and HE staining was applied to observe ovarian tissue structure and count sinus follicles.

6 Research On The Mechanism Of Mucmscs

6.1 Immunohistochemical analysis of ovarian tissue was conducted to detect senescence-related proteins (P53, P16, SOD1), autophagy-related proteins (becline1, LC3b, Sirt1, Sirt3, p62), apoptosis-related proteins (Bax, Bcl-2, Caspase-3), and the expression level of the granular cell-specific protein FSHR.

6.2 TUNEL staining was performed to observe apoptosis in ovarian tissue

6.3 qRT-PCR detection of ageing-related genes (P53, SOD2), autophagy-related genes (becline1, LC3b, Sirt1), apoptosis-related genes (Bax, Bcl-2, Caspase-3) and peroxidase genes (PRDX I, PRDX IV, PRDX V, PRDX VI) was performed.

6.4 Sequencing of mouse ovarian granulosa cell transcriptome: Smart-seq2 technology was used to sequence the mRNA of C57 mouse ovarian granulosa cells, and the bioinformatics method was used to statistically analyse the sequencing data to find differentially expressed protein-coding genes and pathways.

6.5 C57 mouse primary mGCs were cultured to the P1 generation and induced with H_2O_2 at a concentration of 1 mmol / L for 4 h. An oxidative stress model was established with mGCs, and the model cells were co-cultured with mUCMSCs in a transwell plate. mGCs were cultured in the lower

chamber, and mUCMSCs were cultured in the upper chamber. Apoptosis and cellular reactive oxygen species (ROS) levels were measured in a quantitative manner, and the transcription levels of the apoptosis-related gene Bax and anti-apoptotic gene Bcl-2 were detected by qRT-PCR.

7 Statistical Analyses

All statistical analyses were performed using SPSS 21.0 statistical software. Measurement results data are expressed as the mean ± standard deviation. Data for three groups and the above data were analysed using one-way ANOVA. For analysis of differential transcription levels, the negative binomial distribution test was used to test the significance of the differentially expressed genes for the Reads value, and the GO analysis and the KEGG pathway analysis were used to test the significance of the differential gene enrichment using the hypergeometric distribution test. $P < 0.05$ was considered to indicate a significant difference.

Conclusions:

1. The ovarian volume in C57 mice conventionally raised to 18 months decreases, the level of INH-B decreases, and follicles at all levels disappear, and thus, the mice can be used as a model for studying ovarian ageing.

2. mUCMSCs with high purity, strong proliferation activity and multidirectional differentiation potential were obtained using the tissue block attachment method.

3. After treatment of ovarian ageing in mice via mUCMSC transplantation, the ovary volume in the mice increased, follicles at all levels were visible in the cortex, the sinus follicle counts increased, and serum E2, AMH, and INH-B levels increased, indicating that ovarian reserve function was significantly improved. Thus, mUCMSCs have a curative effect on ovarian ageing.

4. mUCMSCs downregulate the expression of apoptosis-related genes (Bax, Caspase − 3) and upregulate the expression of SOD2 and the peroxidase gene PRDX IV, while reducing the granulocyte apoptosis rate and ROS level. Gene expression that regulates anti-inflammatory activity, upregulation of the intracellular phosphatidylinositol kinase-serine / threonine kinase (PI3K-Akt) and P53 signalling pathways, upregulation of cell population proliferation, and IGF-linked proteins (IGFBPs) associated with insulin-like growth factor (IGF) transport and uptake plays a role in promoting repair of the ageing ovary.

5. An oxidative stress model was successfully established in mGCs. Co-culture with mUCMSCs can increase the ability of mGCs to resist oxidative stress and reduce mGC apoptosis.

Abbreviations

mouse umbilical cord mesenchymal stem cells (mUCMSCs); granulocytes (mGCs); assisted reproductive technology (ART); reactive oxygen species (ROS); human umbilical cord mesenchymal stem cells (hUCMSCs); hepatocyte growth factor (HGF); vascular endothelial growth factor (VEGF); insulin-like growth factor-1 (IGF-1); human amniotic mesenchymal stem cells (hAMSCs); Mesenchymal stem cells (MSCs); Umbilical cord mesenchymal stem cells (UCMSCs); inhibin B (INH-B); anti-Müllerian hormone (AMH); Principal component analysis (PCA); insulin-like growth factor binding proteins (IGFBPs); oestradiol (E2); follicle maturation hormone (FSH); follicle stimulating hormone receptor (FSHR).

Declarations

• Ethics approval and consent to participate

Experimental protocols were approved by the Experimental Animal Ethics Committee of the 920th Hospital of the PLA Joint Logistics Support Force.

• Consent for publication

Not applicable.

• Availability of data and material

All data generated or analysed during this study are included in this published article.

• Competing interests

The authors declare that they have no competing interests.

• Funding

This work was supported by grants from the Yunnan Science and Technology Plan Project Major Science and Technology Project (2018ZF007), the Yunnan Province Applied Basic Research Program Key Project (2018FA041, 2017FA040), and 920th Hospital of the PLA Joint Logistics Support Force In-hospital technology plan (2019YGB17, 2019YGA05).

Authors' contributions

XJZ, XMC, GPR and XY made substantial contributions to study conception and design, data acquisition, or data analysis and interpretation.

JZ and JH agree to be accountable for all aspects of the work and ensure that questions related to the accuracy or integrity of any part of the work will be appropriately investigated and resolved.

XHP and GPR have given final approval of this version of the manuscript for publication.

GPR, XHP, XJZ, XQZ and RQP have been involved in drafting the manuscript or revising it critically for important intellectual content.

All authors read and approved the final manuscript.

Acknowledgements

We thank American Journal Experts for assisting with the preparation of this manuscript.

References

1. Leridon H. Demographic effects of the introduction of steroid contraception in developed countries. Hum Reprod Update. 2006;12:603–16.
2. te Velde ER, Pearson PL. The variability of female reproductive ageing. Hum Reprod Update. 2002;8:141–54.
3. Habbema JD, Eijkemans MJ, Nargund G, Beets G, Leridon H. and E.R. Te Velde.(2009). The effect of in vitro fertilization on birth rates in western countries. Hum Reprod *24*, 1414–1419.
4. Turola E, Petta S, Vanni E, Milosa F, Valenti L, Critelli R, Miele L, Maccio L, Calvaruso V, Fracanzani AL, et al. Ovarian senescence increases liver fibrosis in humans and zebrafish with steatosis. Dis Model Mech. 2015;8:1037–46.
5. Song C, Peng W, Yin S, Zhao J, Fu B, Zhang J, Mao T, Wu H, Zhang Y. Melatonin improves age-induced fertility decline and attenuates ovarian mitochondrial oxidative stress in mice. Sci Rep. 2016;6:35165.
6. da Silva Meirelles L, Caplan AI, Nardi NB. In search of the in vivo identity of mesenchymal stem cells. Stem Cells. 2008;26:2287–99.
7. Maki PM, Freeman EW, Greendale GA, Henderson VW, Newhouse PA, Schmidt PJ, Scott NF, Shively CA, Soares CN.(2010). Summary of the National Institute on Aging-sponsored conference on depressive symptoms and cognitive complaints in the menopausal transition. Menopause *17*, 815–822.
8. Pimenta F, Maroco J, Ramos C, Leal I. Predictors of weight variation and weight gain in peri- and post-menopausal women. J Health Psychol. 2014;19:993–1002.
9. Luderer U. Ovarian toxicity from reactive oxygen species. Vitam Horm. 2014;94:99–127.
10. Li J, Mao Q, He J, She H, Zhang Z, Yin C. Human umbilical cord mesenchymal stem cells improve the reserve function of perimenopausal ovary via a paracrine mechanism. Stem Cell Res Ther. 2017;8:55.
11. Ding C, Zou Q, Wang F, Wu H, Chen R, Lv J, Ling M, Sun J, Wang W, Li H, et al. Human amniotic mesenchymal stem cells improve ovarian function in natural aging through secreting hepatocyte growth factor and epidermal growth factor. Stem Cell Res Ther. 2018;9:55.
12. Li J, Li D, Liu X, Tang S, Wei F. Human umbilical cord mesenchymal stem cells reduce systemic inflammation and attenuate LPS-induced acute lung injury in rats. J Inflamm (Lond). 2012;9:33.

13. Broekmans FJ, Soules MR. and B.C. Fauser.(2009). Ovarian aging: mechanisms and clinical consequences. Endocr Rev *30*, 465–493.
14. Zhang J, Xiong J, Fang L, Lu Z, Wu M, Shi L, Qin X, Luo A, Wang S. The protective effects of human umbilical cord mesenchymal stem cells on damaged ovarian function: A comparative study. Biosci Trends. 2016;10:265–76.
15. Ding C, Zou Q, Wang F, Wu H, Wang W, Li H, Huang B. HGF and BFGF Secretion by Human Adipose-Derived Stem Cells Improves Ovarian Function During Natural Aging via Activation of the SIRT1/FOXO1 Signaling Pathway. Cell Physiol Biochem. 2018;45:1316–32.
16. Andersen CY, Ezcurra D. Human steroidogenesis: implications for controlled ovarian stimulation with exogenous gonadotropins. Reprod Biol Endocrinol. 2014;12:128.
17. Hsueh AJ, Billig H, Tsafriri A. Ovarian follicle atresia: a hormonally controlled apoptotic process. Endocr Rev. 1994;15:707–24.
18. Nakahara T, Iwase A, Nakamura T, Kondo M, Bayasula H, Kobayashi S, Takikawa S, Manabe M, Goto T, Kotani, et al. Sphingosine-1-phosphate inhibits H2O2-induced granulosa cell apoptosis via the PI3K/Akt signaling pathway. Fertil Steril. 2012;98:1001–8 e1001.

Figures

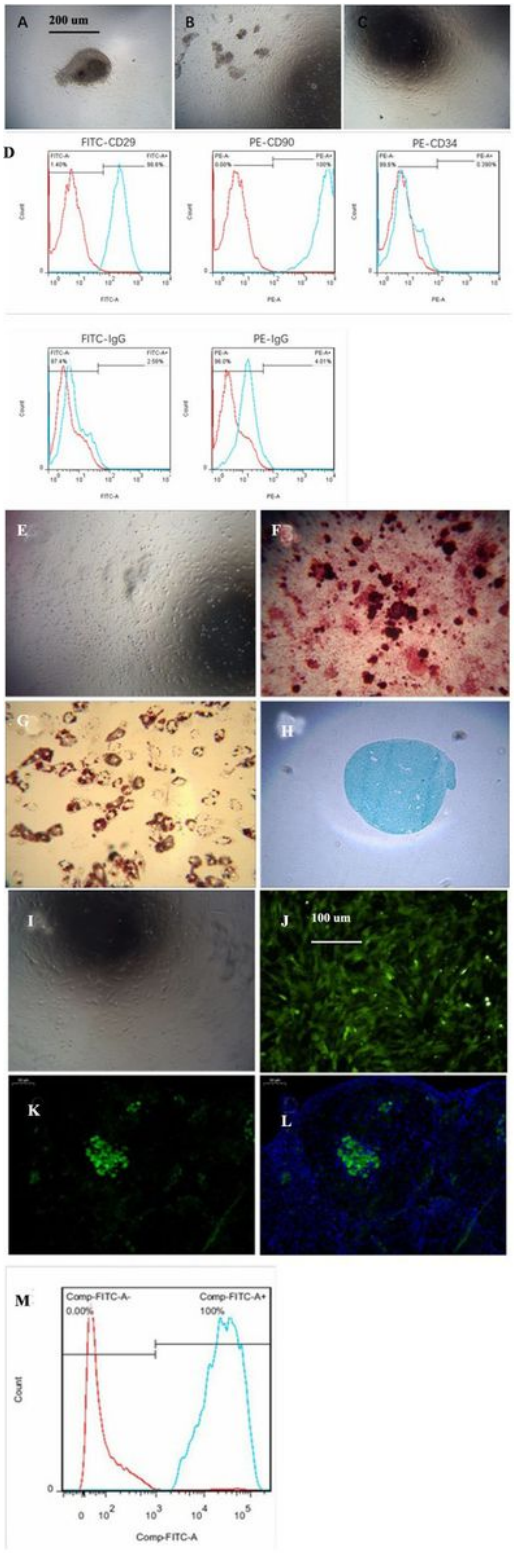

Figure 1

Growth morphology of mUCMSCs (100 ×) A: Primary cell growth morphology on day 1; B: Primary cell growth morphology on day 6; C: P4 cell growth morphology. D: Flow chart of mUCMSCs: The positive expression rates of the cell surface markers CD29, CD90, and CD34 were 98.6%, 100%, and 0.39%. The FITC and PE isotype controls were negative. mUCMSCs were induced to differentiate into osteoblasts, adipocytes and chondrocytes (100 ×) in vitro. E: negative control, F: osteoblast-induced differentiation, G:

adipogenesis-induced differentiation, H: cartilage-induced differentiation. GFP-labelled mUCMSCs (I: 100 ×, J, K, L: 200 ×) I: Morphology of GFP-labelled cells under an optical microscope, J: Morphology of GFP-labelled cells under a fluorescence microscope, K: GFP-labelled cells in ovarian tissue observed via fluorescence microscopy, L: GFP-labelled cells in ovarian tissue observed via fluorescence microscopy after DAPI staining, M: rate of positive mUCMSC labelling with GFP.

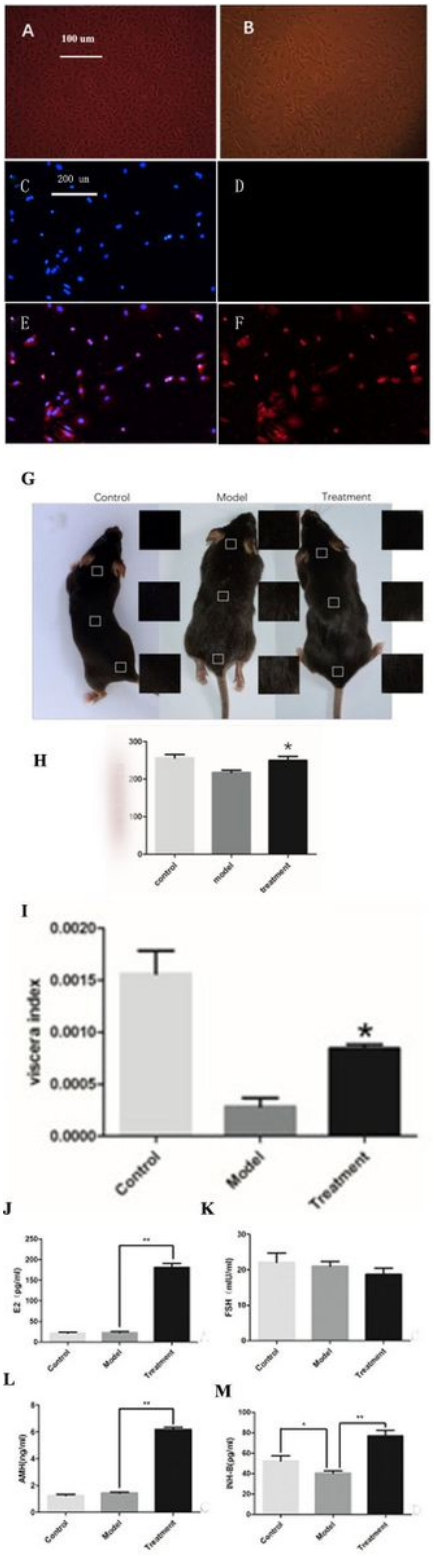

Figure 2

Growth morphology of mGCs (200 ×) A: primary mGCs, B: P1 generation mGCs. Immunofluorescence of mouse ovarian granulosa cells (100 ×) C: negative DAPI staining, D: negative Fluoromount staining, E: DAPI staining with FSHR, F: Fluoromount staining with FSHR. G, H: Grey value change in mouse hair colour: * indicates comparison with model group (P <0.05). I: Statistical chart of mouse ovary index: * indicates comparison with model group (P <0.05). Hormone levels in mouse serum J: mouse serum E2, K: mouse serum FSH, L: mouse serum AMH, M: mouse serum INH-B; * indicates P <0.05, and ** indicates P <0.01.

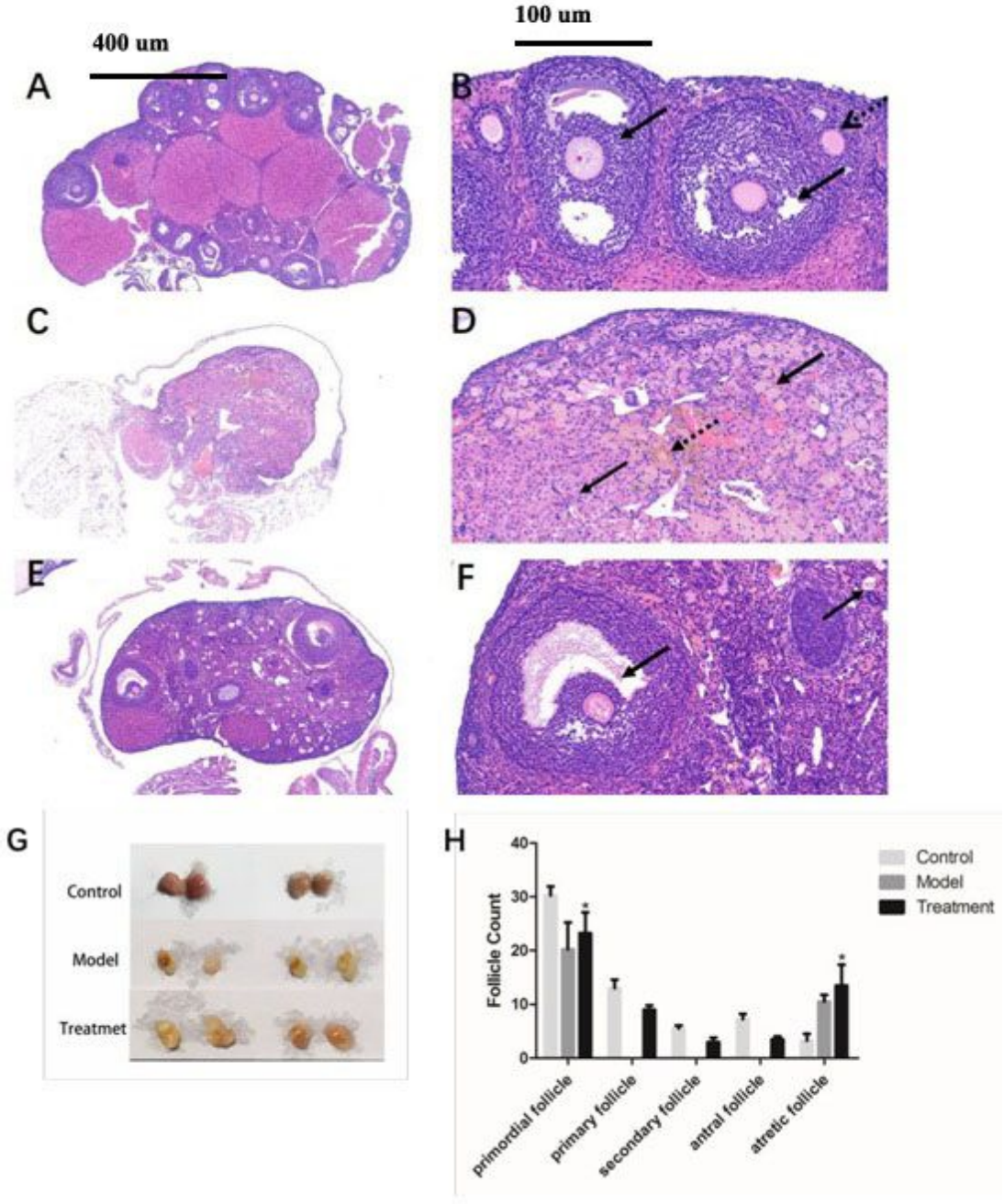

Figure 3

Ovarian tissue structure (A, C, E: 50 ×, B, D, F: 200 ×) A, B: young control group, C, D: model control group, E, F: mUCMSC treatment group, G: Observation of ovaries in each group, H: Follicle counts in each group at various levels; * indicates comparison with the model group (P <0.05).

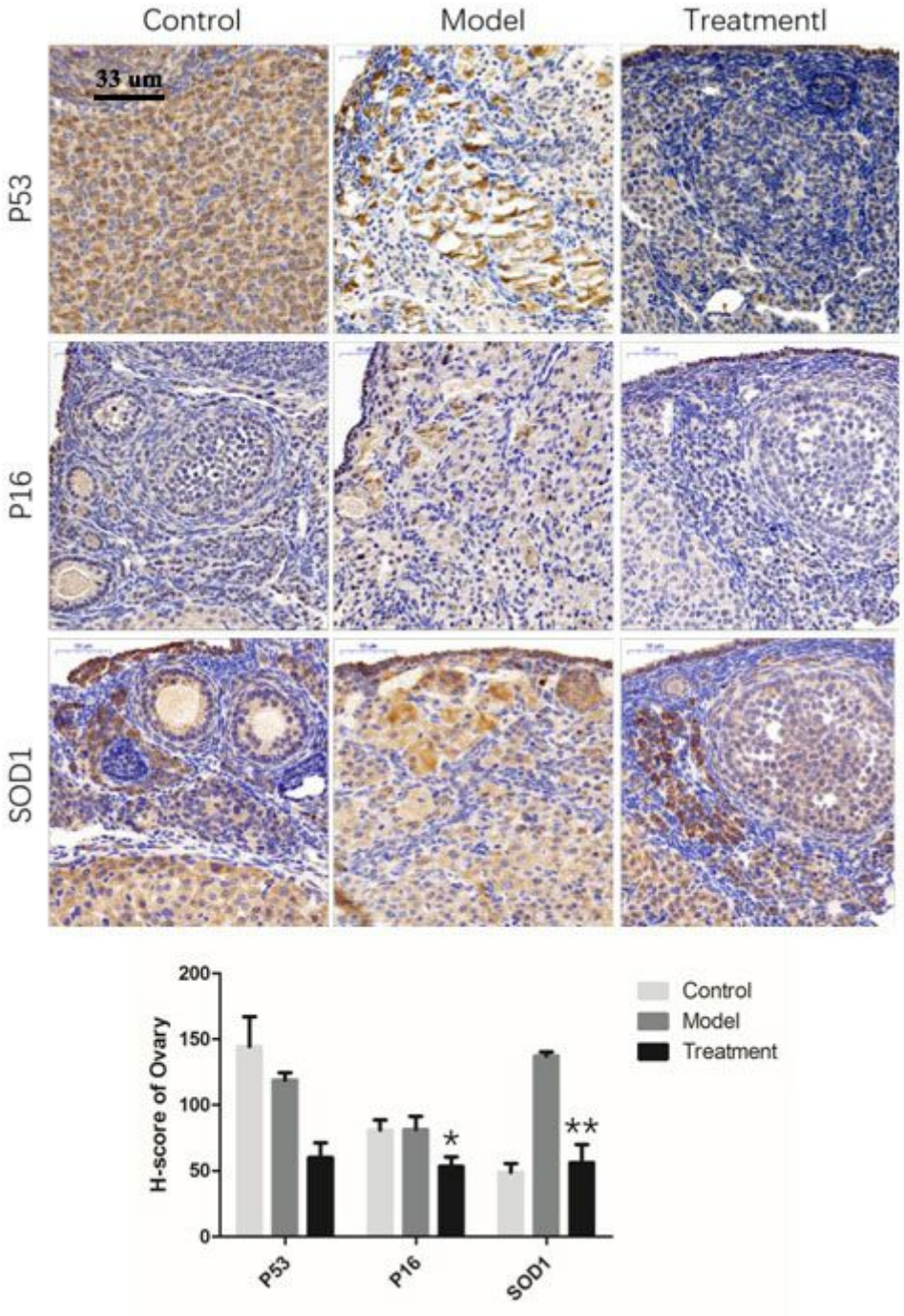

Figure 4

Protein staining and analysis of ovarian ageing-related gene expression (300 ×): * indicates P <0.05, and ** indicates P <0.01.

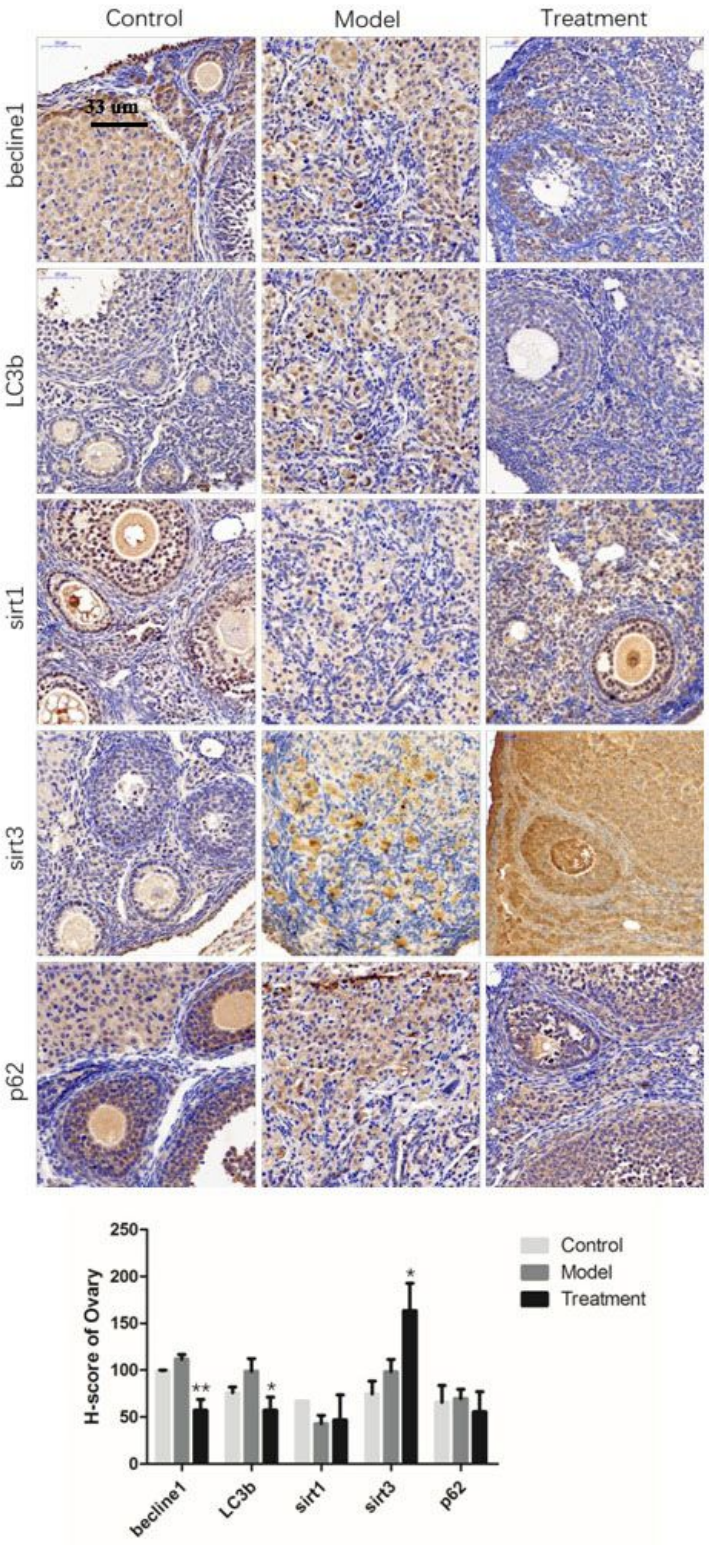

Figure 5

Protein staining and analysis of ovarian autophagy-related gene expression (300 ×): * indicates P <0.05, and ** indicates P <0.01.

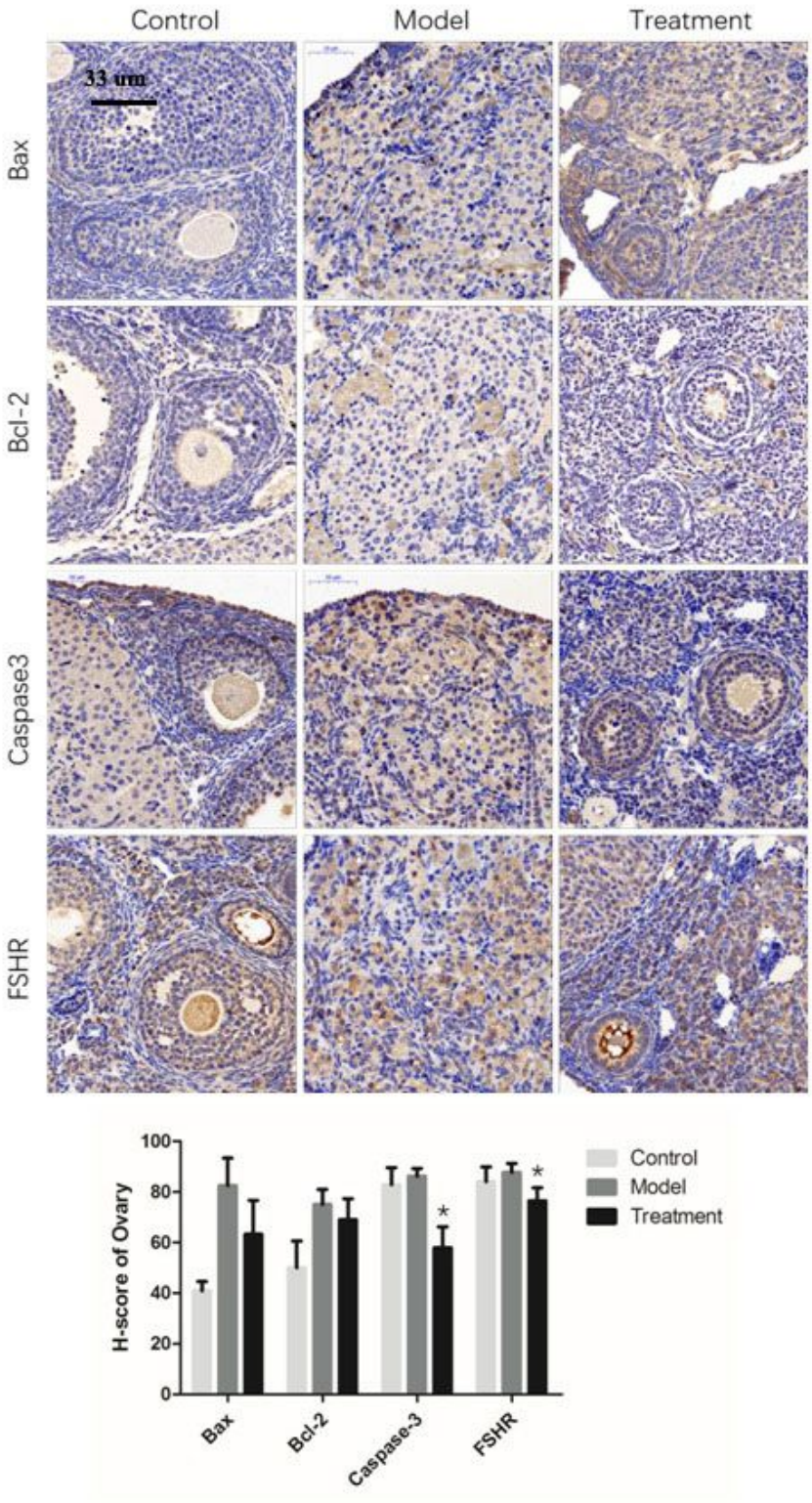

Figure 6

Protein staining and analysis of ovarian apoptosis-related gene expression (300 ×): * indicates P <0.05, and ** indicates P <0.01.

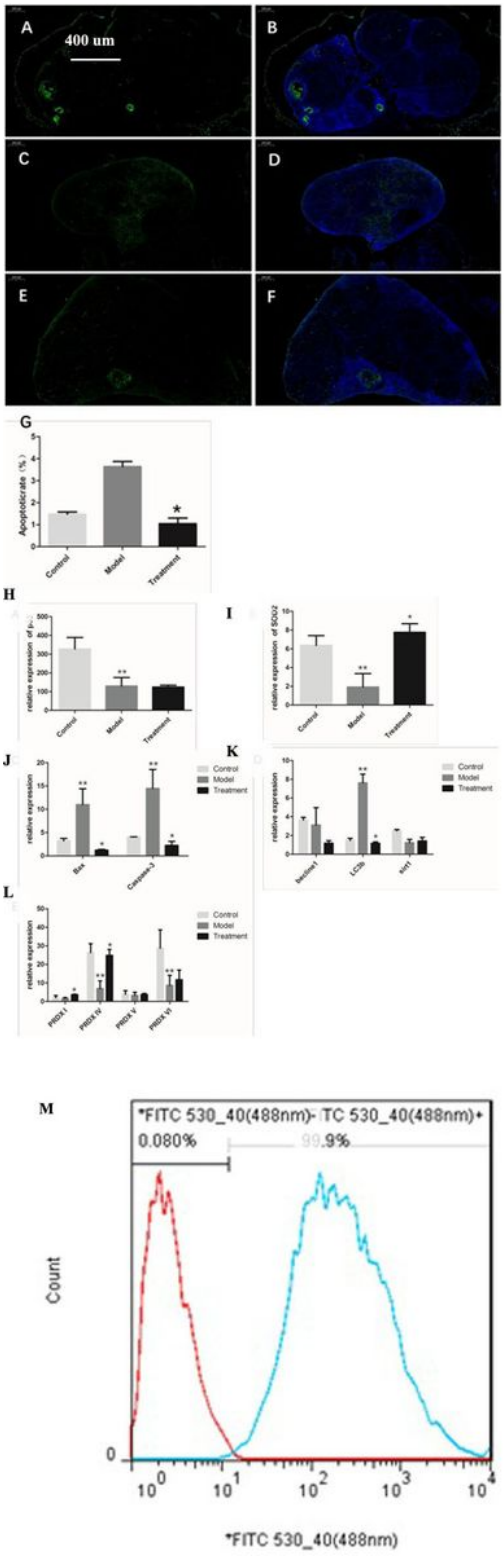

Figure 7

TUNEL staining of ovarian tissue cells (50 ×) A, B: control group, C, D: model group, E, F: mUCMSC treatment group, G: positive rate (i.e., apoptosis rate) statistical chart; * indicates comparison with the model group (P <0.05). H-L: Expression of each gene in ovarian tissue: ** indicates that the model group is compared with the control group (P <0.05); * indicates that the treatment group is compared with the model group (P <0.05). M: positive rate of mouse granular cell sorting.

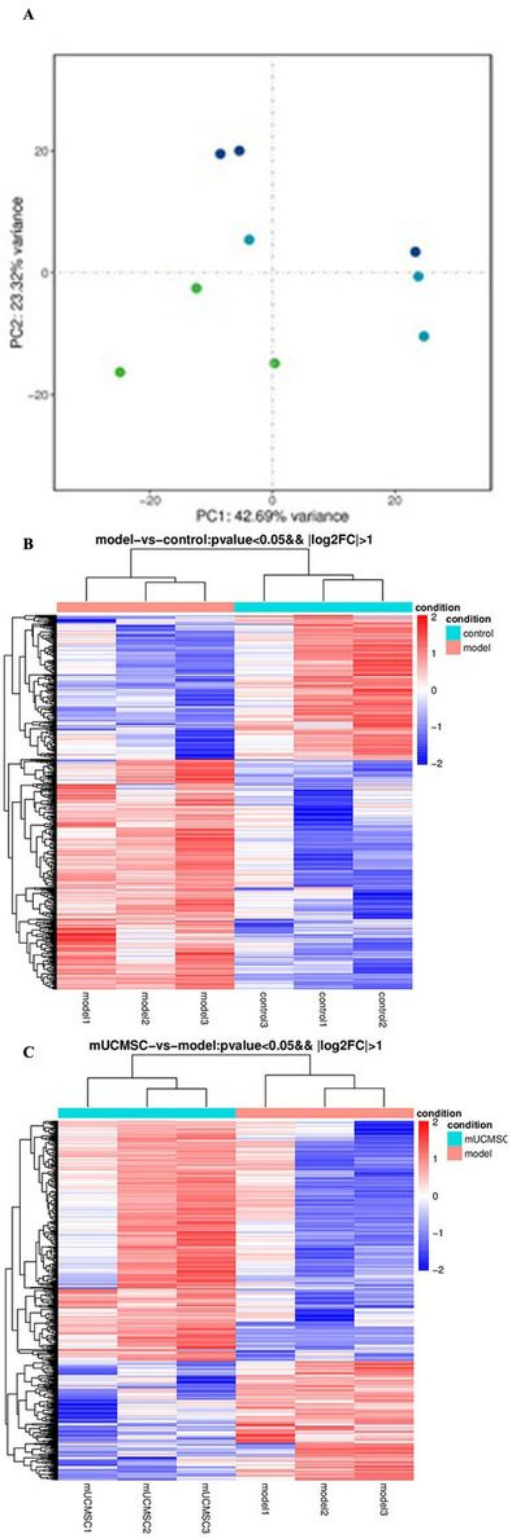

Figure 8

Sequencing results for granular cells. A: PCA Figure: Dark blue indicates the youth control group, light blue indicates the model control group, and green indicates the mUCMSC treatment group. B: Heat map of mRNA cluster analysis of ovarian granulosa cells in the young control group and the model control group: control 1, 2, 3 is the young control group, and model 1, 2, 3 is the model control group. Red in the figure indicates highly expressed genes; blue indicates protein-coding genes with low expression. C: Heat

map of the mRNA clustering analysis of ovarian granulosa cells in the mUCMSC treatment group and the model control group: model 1, 2, 3 is the model control group, and mUCMSC 1, 2, 3 is the mUCMSC treatment group. Red in the figure indicates highly expressed genes. Blue indicates protein-coding genes with low expression.

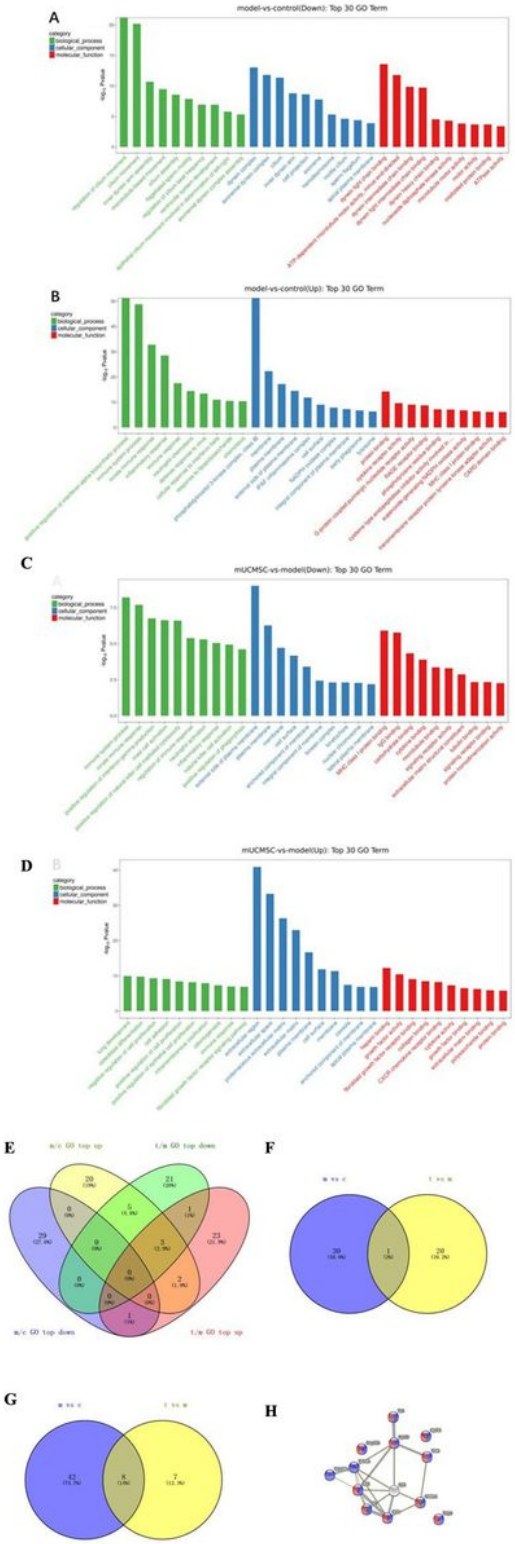

Figure 9

GO enrichment analysis of mRNA of differentially expressed genes in ovarian granulosa cells in the young control group and model control group: A: GO terms downregulated; B: GO terms upregulated. Green indicates GO terms related to biological processes, blue indicates GO terms related to cell components, and red indicates GO terms related to molecular functions. GO enrichment analysis of mRNA of differentially expressed genes in ovarian granulosa cells in the mUCMSC treatment group and the model control group: C: GO terms downregulated; D: GO terms upregulated. Green indicates GO terms related to biological processes, blue indicates GO terms related to cell components, and red indicates GO terms related to molecular functions. E: Common differentially expressed genes between the different comparison groups: m / c represent the comparison between the model control group and the young control group, and t / m represents the comparison between the mUCMSC treatment group and the model control group. F: Common differentially expressed genes involved in immune response items between different comparison groups: m vs c is blue, indicating that the model control group is compared with the young control group, and t vs m is yellow, which indicates that the mUCMSC treatment group is compared with the model control group. G: Common differentially expressed genes involved in inflammatory response items between different comparison groups: m vs c is blue, indicating that the model control group is compared with the young control group, and t vs m is yellow, which indicates that the mUCMSC treatment group is compared with the model control group. H: Inflammatory response entries are commonly involved in the gene string figure: Blue indicates participation in the immune response, and red indicates participation in the inflammatory response.

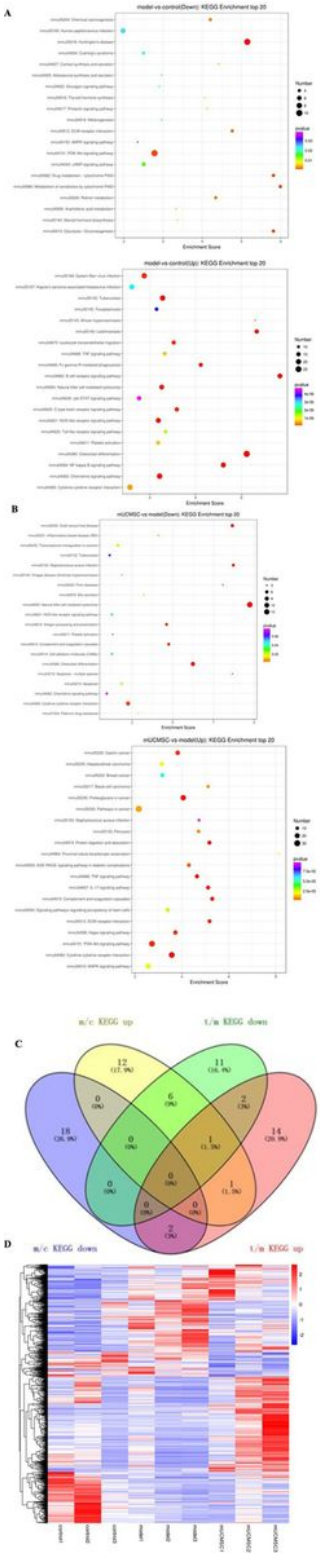

Figure 10

KEGG enrichment of differentially expressed genes in granulocytes A: mRNA KEGG pathway enrichment analysis of ovarian granulosa cells in the young and model control groups: The X-axis Enrichment Score in the figure is the enrichment score, and the bubble colour changes from purple to blue to green to red. The smaller the enrichment p value is, the greater the significance is. B: mRNA upregulation of KEGG pathway enrichment in ovarian granulosa cells in the mUCMSC treatment group and model control group:

The X-axis Enrichment Score in the figure is the enrichment score, and the bubble colour changes from purple to blue to green to red. The smaller the enrichment p value is, the greater the significance is. C: Common differentially expressed genes between different comparison groups. Note: m / c represent the comparison between the model control group and the young control group, and t / m represents the comparison between the mUCMSC treatment group and the model control group. D: Heat map of mRNA cluster analysis of ovarian granulosa cells in the young control group, model control group and mUCMSC treatment group: control 1, 2, 3 is the young control group, model 1, 2, 3 is the model control group, and mUCMSC 1, 2, 3 is the mUCMSC treatment group. Red indicates highly expressed genes, and blue indicates protein-encoding genes with low expression.

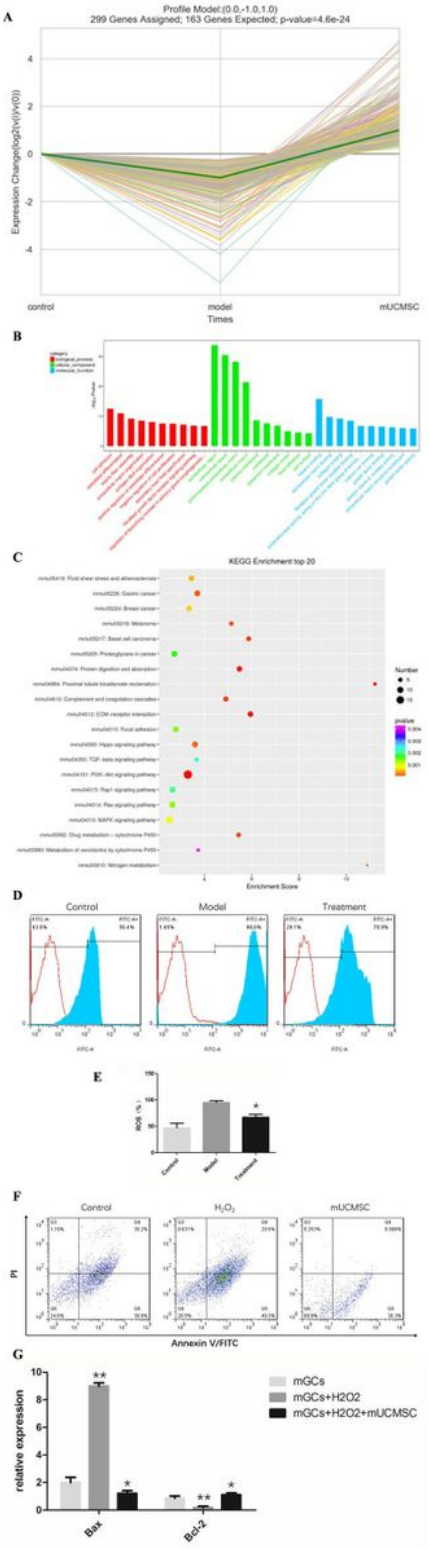

Figure 11

Analysis of Differential Gene mRNA Trends in Three Groups of Granular Cells. A: Trend of 299 differential genes in the three groups in Trend 6. The abscissa control represents the young control group, model represents the model control group, and mUCMSC represents the mUCMSC treatment group. B: GO level 2 distribution map of the top 30 differentially expressed genes in Trend 6. C: top 30 distribution of the gene KEGG analysis in trend 6. D, E: ovarian granulosa cell ROS levels: * indicates comparison with the model

group (P <0.05). F: mouse ovarian granulocyte apoptosis detection: Q4 represents late apoptotic cells, and Q5 represents early apoptotic cells. G: Bax, Bcl-2 transcriptome levels in mouse ovarian granulosa cells: ** indicates that the model group is compared with the control group (P <0.05), and * indicates that the co-culture group is compared with the model group (P <0.05).